Modified self-amplifying RNA mediates robust and prolonged gene expression in the mouse and ex vivo human brain

Authors: Jennifer Freire[1,2*], Joshua E. McGee[1*], Max Heinrich[3], Elijah Hammarlund[3], Sicheng Pang[1], Dana Shaw[1,4], Yuxin Zhou[1], Yangyang Wang[1], Colin Porter[4], Lauren Dang[5], Erynne San Antonio[1], Ziqing Yu[1], Kexin Li[1], Scellig Stone[6], Hart Lidov[7], Jordan Farrell[3,7], Emily K. Osterweil[3,7#], Wilson W. Wong[1, 8#], Mark W. Grinstaff[1,9#] & Xue Han[1#]

[1]Department of Biomedical Engineering, Boston University, Boston, MA, USA.

[2]Department of Pharmacology, Physiology, and Biophysics, Boston, University, Boston, MA, USA.

[3] Rosamund Stone Zander and Hansjoerg Wyss Translational Neuroscience Center and F.M. Kirby Neurobiology Center, Boston Children's Hospital, Boston, MA, USA.

[4]Graduate Program for Neuroscience, Boston University, Boston, MA, USA.

[5]Undergraduate Program for Neuroscience, Boston University, Boston, MA, USA.

[6]Department of Neurosurgery, Boston Children's Hospital, Harvard Medical School, Boston, MA, USA.

[7]Department of Neurology, Boston Children's Hospital, Harvard Medical School, Boston, MA, USA.

[8]Biological Design Center, Boston University, Boston, MA, USA.

[9]Department of Chemistry, Boston University, Boston, MA, USA.

[*]These authors contributed equally: Jennifer Freire, Joshua E. McGee.

[#]Correspondence: xuehan@bu.edu, mgrin@bu.edu, wilwong@bu.edu, Emily.Osterweil@childrens.harvard.edu

ABSTRACT

In self-amplifying ribonucleic acid (saRNA), substitution of cytidine with 5-hydroxymethylcytidine (hm5C) reduces innate immune responses and prolongs protein expression. Administration routes to date for hm5C modified saRNA encapsulated within lipid nanoparticle (LNPs) include intramuscular, as a potent low dose vaccine, but expression levels, patterns, and cell tropism in

other key organs are lacking but critical for advancing RNA treatments/technology. Here we report the protein expression and cell type tropism of modified saRNA-LNPs, encoding fluorescent proteins, when injected in the mouse brain or applied to human cortical brain slices. saRNA encapsulated in an LNP formulation comprising ALC-0315 (present in Comirnaty®) efficiently mediates robust and long-lasting protein expression in mouse brain cells beyond five weeks, with detectable expression in some neurons at three months. hm5C saRNA substantially outperforms N1mΨ mRNA. In addition to transfecting astrocytes and neurons at the injection site, saRNA-LNPs labels neurons retrogradely. Excitingly, the saRNA-LNPs afford robust protein expression in human cortical brain slices, obtained during standard surgical procedures for epilepsy treatment, with expression emerging within twenty-four hours and lasting beyond six days. Thus, saRNA-LNPs are an exciting nonviral gene delivery method that effectively transfects brain cells and will catalyze new opportunities for mechanistic neuroscience research and therapeutic development.

KEYWORDS

Immune evasion, central nervous system, modified saRNA, gene transfer, astrocytes, neurons, human brain slice cultures

SHORT TITLE

Modified saRNA mediates robust and prolonged gene expression in the brain

INTRODUCTION

The ability to genetically modify brain cells is advancing our understanding of the brain and offers exciting therapeutic possibilities[1-4]. While viral transduction remains the most effective method for nucleic acid delivery in the central nervous system, it presents significant limitations in payload capacity and safety concerns for clinical applications. Nonviral ribonucleic acid (RNA) technologies offer promising potential to advance the therapeutic development for neurological and psychiatric diseases[1, 5, 6]. Unlike deoxyribonucleic acid (DNA), messenger ribonucleic acid (mRNA) does not require nuclear entry, thereby eliminating the risk of genomic integration associated with DNA-based methods. The development and successful clinical outcomes of mRNA-based COVID vaccines, which incorporated the groundbreaking discovery of chemically modified nucleotides (N1mΨ) to reduce mRNA immunogenicity and enhance translation efficiency, highlight the potential of mRNA therapeutics.[7-10]

Efforts to deliver mRNA encapsulated in lipid nanoparticles (LNPs) to brain cells demonstrate technical feasibility, though with limited transfection efficiency and a short half-life. For example,

a landmark study in 2001 by Kariko *et al.* reported that injecting mRNA encapsulated in cationic lipofectin into the rat brain leads to immediate protein expression within 1 hour, but the expression becomes largely undetectable after about 24 hours[11]. More recent attempts in delivering mRNA loaded LNPs to brain cells intracerebrally or intraventricularly highlight improved transfection efficiency[12-16], but nonetheless fail to mediate long lasting gene expression due to the inherent limitation of the short half-life of the mRNA transcripts. Finally, the cargo payload capacity of mRNA limits its utility.

Self-amplifying RNAs (saRNAs) encode an RNA-dependent RNA polymerase and replicate themselves inside the cell, resulting in sustained production of protein encoding RNA while providing a large payload capacity (~10k nucleotides). Intracerebral administration of a heme oxygenase-1 encoding wild-type saRNA, encapsulated in deoxycholic acid-conjugated polyethylenimine, affords persistent protein expression for over 7 days in the brain[17]. However, like mRNA, wild-type saRNAs induce innate immune responses. Past attempts to reduce saRNA immunogenicity, including incorporating N1mΨ modification, failed to preserve transfection potency[18-27]. We recently discovered that complete substitution of cytidine with 5-hydroxymethylcytidine (hm5C) and 5-methylcytidine (m5C) reduces immunogenicity and prolongs protein expression. When encoded for the SARS-CoV spike protein and packaged in LNPs, m5C saRNA is a significantly more potent vaccine than conventional N1mΨ mRNA vaccines[28]. Motivated by the improved safety profile and transfection efficiency of modified saRNA, we examined the ability of saRNA-LNPs to transfect brain cells when delivered intracerebrally. We selected hm5C as the modification for saRNA, building upon previous studies that showed efficient transcription and translation[28]. We first screened leading LNPs and identified a formulation comprising ALC-0315 (present in Comirnaty, BioNTech/Pfizer) as the most effective LNP, and then systematically evaluated the time course and cell type tropism of saRNA-LNP mediated fluorescent protein expression in the mouse brain. To demonstrate the translational potential, we additionally tested saRNA-LNPs in ex vivo human brain tissue obtained from epilepsy patients.

RESULTS

ALC0315 containing LNPs effectively deliver saRNA to mammalian brain cells

To evaluate the transfection efficiency of saRNA in the brain, we first screened four leading LNP formulations, comprised of an ionizable lipid, DOPE, cholesterol, and DMG-PEG2K at molar ratios of 50:10:38.5:1.5. The ionizable lipids were SM102 (Spikevax®, Moderna), ALC-0315 (Comirnaty®, BioNTech/Pfizer), L319[29] , and Lipid A9. We loaded hm5C modified saRNA encoding either mCherry or GFP into these LNP formulations. The saRNA-LNPs possessed a size between 100-200nm (Fig. 1B), a polydispersity index <0.2 (Fig. 1C), and an encapsulation efficiency >80% (Fig. 1D). We then intracerebrally injected these saRNA-LNPs into the striatum of mice (625 ng, 5μL at 125 ng/μL, Fig. 1E), and quantified protein expression three days post injection by visualizing cellular fluorescence in brain slices. All LNP formulations, except SM102, mediated prominent fluorophore expression (Fig. 1F-H), with ALC-0315 exhibiting the highest protein expression (Fig. 1F, Hii).

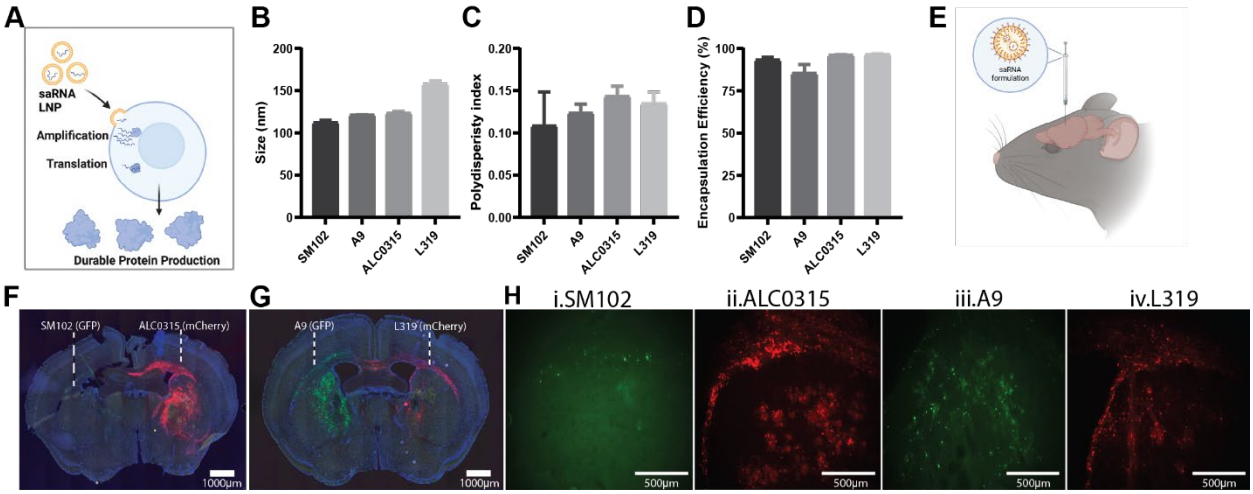

Figure 1. Screening LNPs for efficient saRNA delivery into brain cells. (A) Conceptual illustration of saRNA-LNP mediated protein expression. **(B-D)** Size (B), polydispersity (C), and encapsulation efficiency (D) of LNP formulations comprising SM102, A9, ALC-0315, and L319. **(E)** Illustration of experimental testing in the mouse brain. **(F, G)** Transfection efficiency of the four LNPs loaded with saRNA encoding GFP or mCherry. Shown are GFP (green), mCherry (red) and DAPI (blue) fluorescence at 3 days post saRNA-LNP injection. **(H)** Zoom-in views of F and G showing GFP (green) and mCherry (red) fluorescence.

saRNA-LNPs mediate robust and prolonged gene expression in the brain

To quantify the efficiency and the time course of saRNA-LNP mediated gene expression, we injected the most effective LNP composition comprised of ALC-0315 loaded with saRNA encoding mCherry into the mouse striatum. As a comparison, another cohort of animals received ALC-0315 LNPs loaded with conventional N1mΨ mRNA encoding mCherry (mRNA-LNPs). One day after saRNA-LNP or mRNA-LNP injection, prominent mCherry expression was present around the injection site, which persisted throughout many weeks post injection (Fig. 2A). Surprisingly, mCherry expression was also evident throughout the corpus callosum, suggesting robust labeling of neuronal axons or myelin.

We next estimated the tissue area transduced by manually segmenting the mCherry-positive area around the striatal injection site and throughout the corpus callosum. mCherry expression progressively increased over the first week, with saRNA-LNPs and mRNA-LNPs transfecting similar areas in both the striatum and the corpus callosum within the first three days post injection (Fig. 2B, C), but with mRNA-LNPs transfecting a greater area than saRNA-LNPs at one week. However, mRNA-LNP mediated mCherry expression quickly declined after one week, dropping to nearly undetectable levels in most mice by week four. In contrast, saRNA-LNP mediated expression remained prominent until week five at the injection site and in the corpus callosum. In one animal examined at three months post saRNA-LNP injection, the longest time-point evaluated, robust mCherry fluorescence was present in some neurons, throughout both the soma and neuronal processes (Supp. Fig. 1). The persistent saRNA-mediated transcript expression in neurons, though sparse, even at three months after a single injection further underscore the effectiveness of saRNA mediated neuronal transfection. Together, these results demonstrate that

chemically modified saRNA mediates more robust and prolonged gene expression in brain cells than conventional N1mΨ mRNAs.

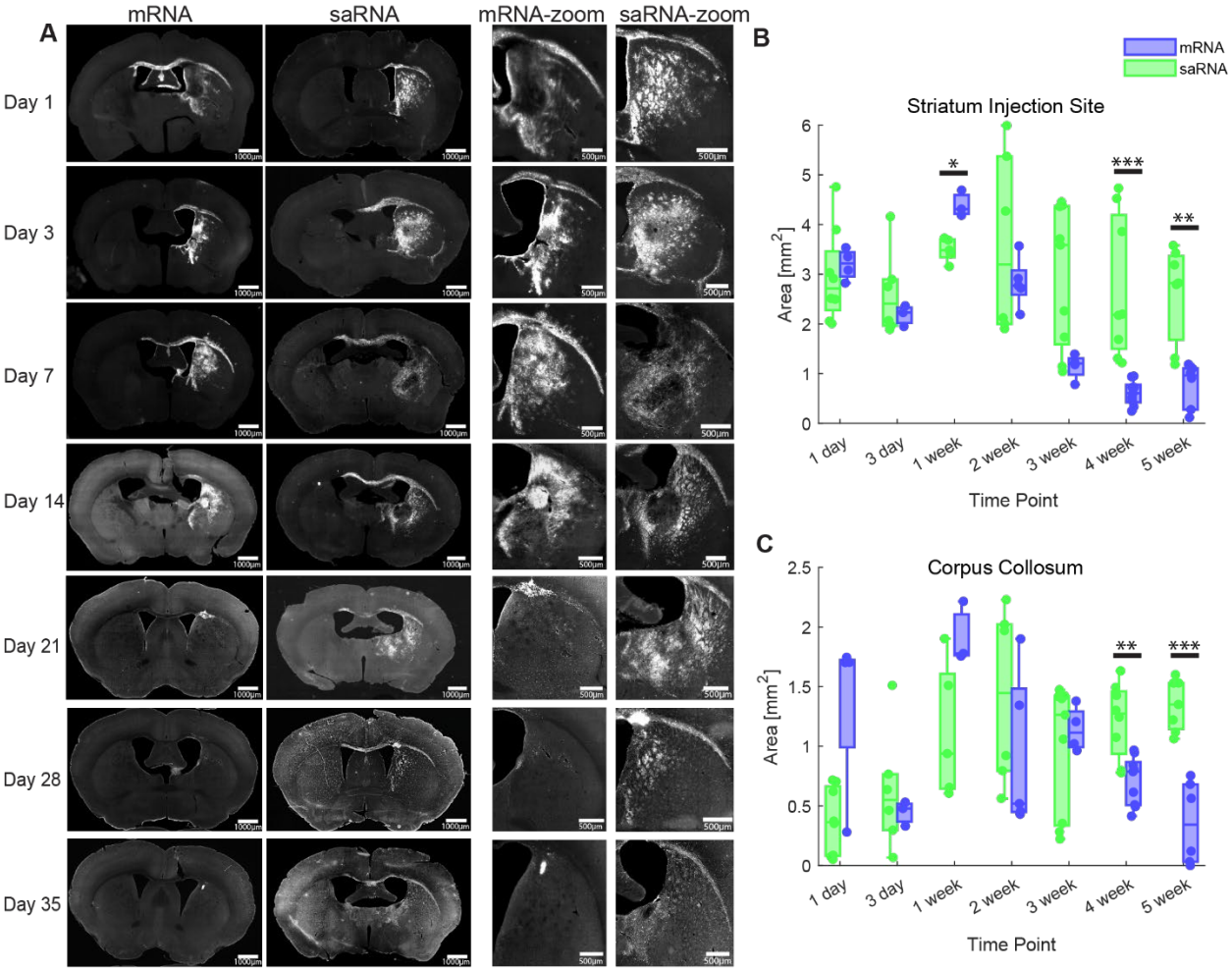

Figure 2. saRNA-LNPs mediate robust and long-lasting gene expression. (A) Example brain slices at days 1-35 post saRNA-LNP injection, showing robust mCherry fluorescence at the site of injection in the striatum. Left, whole brain slices showing injection in the right hemispheres for mRNA-LNPs and saRNA-LNPs. Right, corresponding zoomed-in views. **(B, C)** mCherry+ area around the injection site (**B**) and corpus callosum (**C**) across days post-injection. Shown are box plots (box: 1st and 3rd quartiles, horizontal line: median, whiskers: 1.5x interquartile range). ***, $p<0.005$; **, $p<0.01$; *, $p<0.05$, Wilcoxon rank-sum test (n=2-3 slices per mouse, 2-3 mice per time point).

saRNA-LNPs predominantly transduced astrocytes at the site of injection.

To further analyze the cell types labeled by saRNA-LNPs, we performed immunofluorescence staining using antibodies against the astrocyte marker protein GFAP or the neuronal marker protein NeuN (Fig. 3A-C). As astrocytes do not have a well-defined morphology, we calculated the fraction of mCherry positive (mCherry+) pixels that were also GFAP positive (GFAP+). We found that 43-56% of mCherry+ pixels were GFAP+ across the post injection time points examined. As neurons possess a defined morphology, we computed the fraction of mCherry+

pixels that were part of a neuron (NeuN+). Only ~1-4% of labeled pixels were neurons across the time points examined, significantly lower than astrocytes (Fig. 3D). These results demonstrate that saRNA-LNPs transfect both neurons and astrocytes, with the majority of labeled cells being astrocytes at the striatal site of injection.

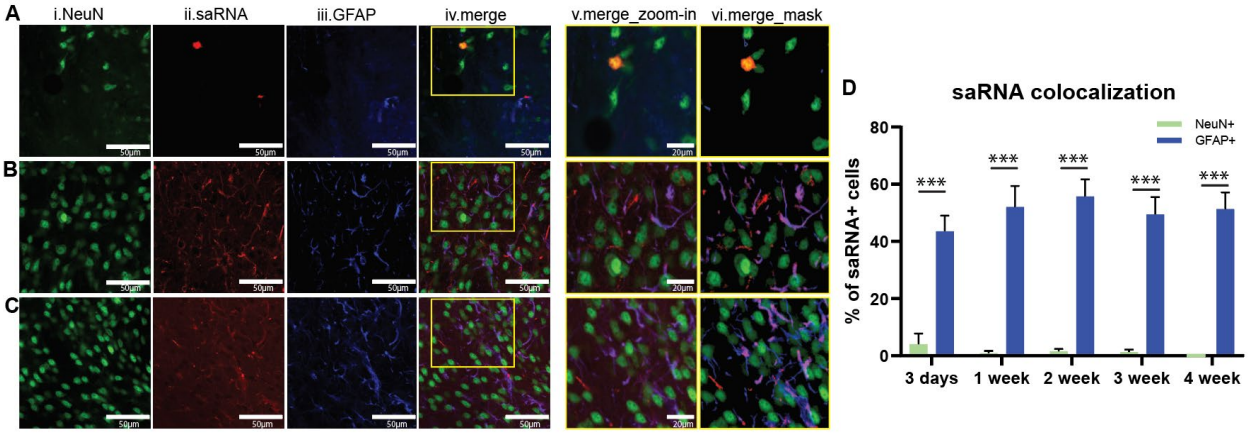

Figure 3. saRNA-LNP transfected more astrocytes than neurons in the striatum. (A) An example brain slice showing saRNA-LNP mediated gene expression in neurons. (i) NeuN immunofluorescence from neurons (green); (ii) saRNA-LNP mediated mCherry fluorescence; (iii) GFAP immunofluorescence from astrocytes (blue); (iv) Merge, showing colocalization of mCherry and NeuN immunofluorescence (orange). (v). zoomed in view of the area highlighted by yellow box in iv. (vi). Cell profiler identification of pixels positive for NeuN (green), saRNA (red), and GFAP (blue). **(B, C)** Similar to **A**, but for example brain slices showing saRNA-LNP mediated gene expression in astrocytes. Merge showing colocalization of mCherry and GFAP immunofluorescence (purple). **(D)** Quantification of the percentage of saRNA-mediated mCherry expression colocalization with neurons (green) versus glia (blue) across 5 time points after saRNA injection. ***, $p<0.001$, Wilcoxon rank-sum test (n=10-19 fields of view per timepoint).

saRNA-LNPs mediates potent retrograde labeling of cortical neurons projecting to the striatal injection site

In addition to robust expression at the site of injection, we noticed that mCherry+ neurons were prominent in the cortex starting about two weeks post injection (Fig 4A-C). Many labeled neurons exhibited bright mCherry fluorescence throughout the cell bodies, and the proximal and distal processes (Fig 4C), suggesting that saRNA-LNPs retrogradely label cortical neurons projecting to the striatal injection site.

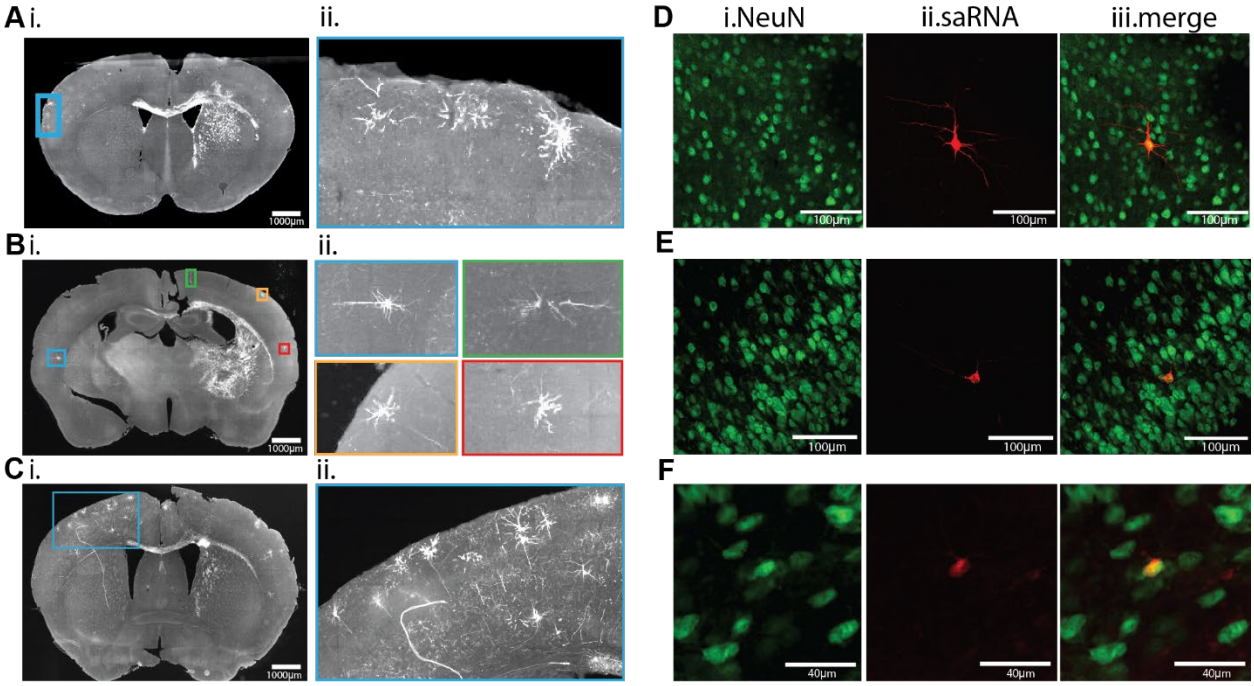

Figure 4. saRNA-LNPs retrogradely label cortical neurons. (A)(i) An example brain slice at 2 weeks post injection. (ii) A zoomed-in view of labeled cortical neurons highlighted by the blue box in A. **(B)** An example brain slice at 3 weeks post injection. (ii) Zoomed-in views of labeled cortical neurons across different areas of the cortex highlighted in blue, green, yellow, and red boxes in **B**. **(C)**(i) An example brain slice at 4 weeks post injection. (ii) Zoomed-in view of labeled cortical neurons highlighted by blue box in **C**. **(D-F)** Example fields of view showing saRNA-LNP mediated gene expression in cortical neurons. (i) NeuN immunofluorescence from neurons (green); (ii) saRNA-LNP mediated mCherry fluorescence (red); (iii) Merge, showing colocalization of mCherry and NeuN immunofluorescence (yellow).

saRNA-LNPs mediate robust mCherry expression in human cortical brain slices

To explore the translational potential of saRNA, we applied 4µL of saRNA-LNP onto each human cortical brain slice (**Methods**). Confocal imaging of slices showed robust mCherry expression at 24 hours post saRNA-LNP application in the frontal cortex, both the superficial layer and deep layer, of a 3-month-old male patient (Fig. 5A). Almost all mCherry positive cells had neuronal morphology, suggesting a strong tropism towards neurons, distinct from the early astrocyte tropism observed in mouse striatum. Similarly strong expression was also detected at 6 days post-application in the deep layer of a temporal cortex slice of a 14-month-old male patient (Fig. 5B). Curiously, we did not observe any expression in the frontal brain slices of a 3-year-old male patient or the temporal cortex slices from a 21-year-old female patient. Thus, saRNA mediates robust gene expression in human cortical brain tissue, with a rapid expression onset within 24 hours of application and lasting beyond 6 days, highlighting the exciting translational potential of saRNA mediated gene transduction.

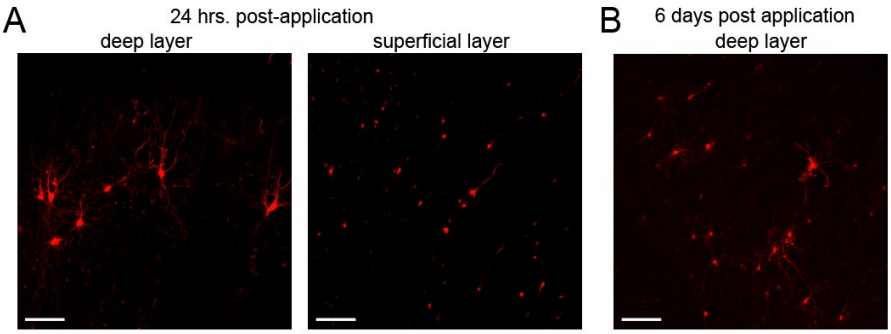

Figure 5. saRNA-LNPs mediate robust gene expression in surgically resected human brain tissue. (**A**) Brain slice from the deep (left) and superficial (right) layers of frontal cortex of a 3-month male patient. Images acquired at 2 days in vitro (DIV), 24 hours post saRNA-LNP application. (**B**) Brain slice from the deep layer of the temporal cortex of a 14-month male patient. Image acquired at 7 DIV, 6 days post saRNA-LNP application. Scale bars are 200 μM

DISCUSSION

Motivated by the exciting progress in the durable expression previously observed from modified saRNA-based vaccine technology, we examined the transfection efficiency of modified saRNA encapsulated in LNPs following intracerebral delivery in the mammalian brain. Our results show that saRNA-LNPs potently transfect brain cells at the injection site in the striatum region, and across broad cortical areas that project to the striatal injection site. hm5C saRNA-LNPs afford robust and prolonged mCherry transcript expression beyond five weeks, with some neurons remaining mCherry positive at three months post-delivery, the longest time-point examined. hm5C saRNA yields significantly longer lasting protein expression than conventional modified mRNAs. Intriguingly, while hm5C saRNA-LNPs predominantly label astrocytes at the site of injection, many cortical neurons are also retrogradely labeled.

We tested four leading LNP formulations, identified in previous work, that exhibit excellent transfection efficiency in human and mouse cell lines. Formulations of SM102 (Spikevax®, Moderna) and ALC-0315 (Comirnaty®, BioNTech/Pfizer) effectively transfect muscle cells when formulated as vaccines. However, their transfection efficiency in the brain varies drastically, with SM102 transfecting a few cells, whereas ALC-0315 is the most potent, highlighting the distinct tissue tropism of different LNP formulations.

Recent advances in designing ionizable LNPs yield improved mRNA delivery, particularly in vaccine development, offer promising potential for optimizing LNP-based non-viral gene transfection strategies for other tissues[1, 6, 30-33]. Ionizable lipids play a critical role in determining the physicochemical properties and delivery performance of the formulated LNP-mRNA. A screen of ionizable lipid based on polyamines with different alkyl tail length reveals a composition with mRNA that exhibits 17-fold greater fLuc expression in the fetal mouse brain at 4 hours compared to DLin-MC3-DMA LNPs (MC3) [14]. An alternative approach incorporates an ionizable lipid

conjugated to tryptamine, which binds trace amine-associated receptors expressed in the brain. An intrathecal injection of this resulting LNP-mRNA, encoded with fLuc, outperforms the MC3 LNP-mRNA formulation with a 42-fold greater luminescence intensity at 6 hours[15]. Additionally, *in vitro* high-throughput screening activities are identifying LNPs with improved blood brain barrier penetration capabilities[34], and enhanced tissue and cell specificity[35]. Aside from engineering LNPs to enhance mRNA delivery, incorporation of 3'UTR gene regulatory elements in the sequence to bias gene expression between astrocytes and neurons is also an exciting strategy to further control translation[36]. Continued efforts on engineering LNP formulations and mRNA/saRNA sequence designs will further improve transfection efficiency, cell type specific targeting, and brain specific targeting.

Our data demonstrates that modified hm5C saRNA robustly expresses mCherry protein for over five weeks after a single injection in the striatum, with mCherry fluorescence remaining prominent in some neurons even at three months post injection. This is well beyond the expression mediated by mRNA previously tested[11-16], or the seven days reported in a previous study using wild-type saRNA[17]. Importantly, we directly measured mCherry expression via microscopy. This is in sharp contrast to previous studies that reported a Cre-mediated recombination process triggered by mRNA-mediated expression of Cre transcripts[14, 15, 32], which amplifies the transient presence of Cre into a more permeant recombination readout and thus cannot characterize the time course or the actual amount of mRNA transcripts.

At the striatal injection site, the hm5C saRNA-LNPs predominantly label astrocytes and a few neurons. The robust astrocyte labeling is generally in agreement with the study by Tuma et al., which showed that intracerebral injection of mRNA encoding Cre led to robust recombination-mediated astrocyte labeling in the striatum[32]. However, they observed similar labeling of astrocytes and neurons in the striatum, in contrast to the low expression observed in striatal neurons we find. As the Cre-dependent recombination assay captures transient Cre-enzyme expression, the discrepancy in transgene expression observed may reflect the time course or the magnitude of variations between our study and Tuma *et al*. Indeed, the retrograde labeling of cortical neurons appears to progressively become stronger over the first couple of weeks, suggesting that saRNA transcripts may accumulate slower in neurons than in astrocytes, leading to the observed low protein expression at the site of injection. However, it is also possible that ALC-0315 LNPs exhibit a low transfection rate for the medium spiny neurons that dominate the striatal neuron population. Lastly, similar to the low microglial labeling reported previously[32, 37], we only detected very limited instances of mCherry positive microglia labeled by our hm5C saRNA-LNPs (Supp. Fig. 2). It is surprising to detect robust retrograde labeling of cortical neurons that project to the striatum injection sites, including contralateral to the injection site. Such retrograde labeling may explain the prominent expression of mCherry observed in the corpus callosum, though it is possible that myelin may be the dominant source of the corpus callosum labeling.

An important step towards translation is the verification that saRNA-LNP can effectively express in human brain tissue. To test this, we applied saRNA-LNP to living slices prepared from resected cortical tissue obtained during pediatric epilepsy surgery at Boston Children's Hospital. We observed expression of mCherry in as little as 24 hours, which lasted for at least 6 days. This robust expression was seen in slices from tissue collections from two separate patients. Given

the rapid and stable nature of the expression, saRNA-LNP could be a valuable method for gene delivery, but future studies will need to systematically quantify the expression stability across longer timescales and assess the effect of age and underlying pathology on saRNA mediated gene expression in the human brain.

hm5C saRNA's ability to mediate long-term gene expression in brain cells, in both mouse and human brain slices, presents profound therapeutic potential, e.g., to deliver glial derived neurotrophic factors for Parkinson's disease[38], brain-derived neurotrophic factor for Alzheimer's disease[36], Bcl-2 for ischemic stroke[2, 39], apoptosis-inducing ligand for glioblastoma[40], and thrombomodulin to boost blood brain barrier integrity[41]. Additionally, continued progress to improve nonviral delivery of antisense RNA, siRNA, or CRISPR-Cas9 gene editing components into the brain will advance the ability to reduce risk factors of many neurological and psychiatric disorders[1], e.g., beta-secretase 1 or amyloid beta for Alzheimer's disease[42-45], alpha-synuclein for Parkinson's disease[46, 47], SOD1 for Amyotrophic lateral sclerosis[48], or as an immunotherapy for glioblastoma[49, 50]. Thus, hm5C saRNA-LNP represents a potent non-viral gene transduction platform for the mammalian brain with broad applicability in basic neuroscience research and exciting translational potential.

METHODS

saRNA & mRNA LNP synthesis

Both saRNA and mRNA encoding mCherry or EGFP were synthesized by *in vitro* transcription with the T7 High Yield kit (New England Biolabs). For the saRNA constructs, cytidine was replaced by 5-hydroxymethyl (TriLink). For the mRNA constructs, uridine was replaced by N1-methylpseudouridine. Following transcription for 3 hours at 37 °C, the DNA templates were digested by TurboDNase (Invitrogen). The RNA preparations were purified using the Monarch RNA KPurification kit (New England Biolabs) and eluted in water. Additionally, cellulose purification was performed as previously described to remove double-stranded RNA contaminants.[51]

The hm5C saRNA and N1mΨ mRNA encoding mCherry or EGFP were encapsulated into LNP formulations using ionizable lipids including ALC-0315 (Avanti), SM102 (Cayman), Lipid A9 (Cayman), or L319 (Cayman), in combination with DOPE (Avanti, 850725), Cholesterol (Avanti, 700100), and DMG-PEG2K (Avanti, 880151) at molar ratios of 50:38.5:10:1.5. RNA was incorporated at an N:P ratio of 10. Following encapsulation, the LNPs were dialyzed in sterile 1X Phosphate-buffered saline (PBS) overnight at 4°C. Particle size was determined via dynamic light scattering using a NanoBrook Omni (Brookhaven Instruments). Encapsulation efficiency and RNA concentration were measured with the Quantifluor RNA System (Promega). The LNPs were then concentrated with a 3 kDa MWCO Amicon Ultra Centrifugal filter to approximately 200 ng/μL and further diluted to 125ng/μL with sterile PBS. LNPs were either stored at 4˚C and administered within 3 days of preparation or stored at -20˚C until use.

Animal experiment

All animal procedures were approved by the Boston University Institutional Animal Care and Use Committee (IACUC). Male and female adult C57BL/6 mice (Jackson Labs or Charles River Laboratory) were used, and their ages were 2-5 months at the start of the experiment. During aseptic stereotaxic surgery, mice were anesthetized with isoflurane (5% for induction, 2% or less for maintenance) and preoperatively injected with sustained release buprenorphine (Ethiqa XR). LNPs loaded with saRNA or mRNA (625 ng total, 5μL at 125 ng/μL) were infused into the striatum through a small craniotomy at 3 depths (ML: -1.8mm, AP: +0.5mm, and 2μL at -2.8mm, 2μL at -2.5mm, and 1μL at -2.2mm), at a rate of 100-250 nL/min via a 10μL syringe (Hamilton Company). At the completion of all 3 infusions, the Hamilton syringe was kept in place for an additional 10 minutes before being retracted. Vetbond tissue adhesive (3M Inc) was then applied to close the incision.

Histology and immunostaining

Mice were transcardially perfused with PBS followed by 4% paraformaldehyde (PFA) buffered in PBS. Brains were collected, post-fixed in 4% PFA-PBS overnight at 4℃, and transferred to a solution with 30% sucrose in PBS at 4℃ until sinking. Brains were then sliced coronally at 50μm thickness using a freezing microtome (Leica, SM2010R) or cryostat (Leica, CM3050S). To assess the efficiency and the time course of saRNA-LNP mediated gene expression, we performed whole-slice imaging using an Olympus VS120 slide scanner microscope at 20X magnification to visualize mCherry fluorescence.

To quantify neuronal versus astrocyte targeting, we selected 2-3 sections positive for mCherry from each mouse at each desired time point using a fluorescence microscope (Leica, DFC365 FX). The selected tissue sections were then incubated in sodium citrate buffer (10mM, 6.0 pH; Sigma Aldrich, W302600) at 37℃ for 1 hour, and then transferred into a blocking solution (5% goat serum and 0.5% TritonX-100 in PBS) to prevent non-specific protein binding for 1 hour. Sections were then incubated with primary antibodies against neuronal nuclei, NeuN (rabbit, 1:500; Abcam, ab177487) and glial fibrillary acidic protein, GFAP (chicken, 1:1000; Novus Biologicals, NBP1-05198) at 4℃ overnight followed by secondary antibodies Alexafluor 488 goat anti-rabbit (1:500; Invitrogen, A11008) and Alexafluor 647 goat anti-chicken (1:500; Invitrogen, A21449) for 2 hours at room temperature. Slices were then mounted using Vectashield antifade mounting medium with DAPI (Vector Laboratories, H-1200). Immunofluorescence was then acquired using an Olympus FV3000 confocal microscope at 40X magnification and 2x zoom.

Image analysis

Colocalization analysis was performed using open-source software *CellProfiler (https://cellprofiler.org/)*. Specifically, TIFF images were loaded in CellProfiler as single-channel grayscale images, which were manually thresholded to generate masks corresponding to NeuN positive neurons, GFAP+ glia, or mCherry+ positive objects. As neurons have defined

morphology, we applied an additional filter that was optimized by manually adjusting the object area and formfactors to capture the standard shapes of neurons across all NeuN+ neurons. False positive pixels were defined as those positive for more than one marker (NeuN, GFAP, or mCherry). False positive pixels were removed from all subsequent calculations. To compute the labeling specificity of saRNA in astrocytes, we computed the ratio of pixels positive for both mCherry and GFAP over pixels positive for mCherry. To compute the labeling specificity of saRNA neurons, we computed the ratio of pixels positive for both mCherry and NeuN over the pixels positive for mCherry.

To estimate the area of RNA-mediated mCherry expression, we first manually identified the slice with the highest mCherry fluorescence in each mouse, then selected two adjacent slices. Two experimenters, blind to experimental conditions, independently segmented the areas positive for mCherry in MATLAB. As the segment areas in each slice were largely identical between the two experimenters, the mean area segmented by the two experiments was used for each slice.

Human cortical tissue experiment

Human cortical tissue was obtained by informed consent in collaboration with the Repository Core for Neurological Disorders within the Rosamund Stone Zander and Hansjoerg Wyss Translational Neuroscience Center, Boston Children's Hospital, which is also supported by the IDDRC (NIH P50HD105351). Samples used in this study were either temporal or frontal cortex, collection from macroscopically normal non-lesional cortex obtained in the course of epilepsy surgery.

Immediately following resection, samples were directly placed in carbogenated ice-cold slicing artificial cerebral spinal fluid (ACSF) (80mM NaCl, 75 mM Sucrose, 2.5mM KCl, 1.25mM NaH_2PO_4, 26mM $NaHCO_3$, 10 mM D-glucose, 0.5mM $CaCl_2$, 7mM $MgCl_2$, 1.3mM sodium ascorbate, 3.0 mM sodium pyruvate, 1x Penicillin-Streptomycin (Thermo Fisher, 15140122), and 3U/mL Nystatin (Sigma-Aldrich, N1638)) and transported to lab under 15 min. 300 µm thick slices were prepared using a Leica VT1200S vibratome and transferred into a recovery solution (HBSS supplemented with 20mM HEPES, 1 x Penicillin-Streptomycin, and 3U/mL Nystatin, at pH 7.3) at room temperature saturated with 95% O2 5% CO2. After 30min recovery at room temperature, slices were transferred onto Millicell 6-well culture inserts (Millipore PICM0RG50) in culture media (96% (v/v) BrainPhys (StemCell Technologies, 5790), 2.6 mM calcium chloride, 2.6 mM magnesium chloride, 1x N-2 Supplement (Thermo Fisher, 17502001), 1x B-27™ Supplement serum-free (Thermo Fisher, 17504044), 1x Penicillin-Streptomycin (Thermo Fisher, 15140122) 3U/mL Nystatin (Sigma-Aldrich, N1638), 2 µM ascorbic acid, 10 mM D-Glucose, 20ng/mL human recombinant BDNF (StemCell Technologies, 78005), 20ng/mL human recombinant GDNF (StemCell Technologies, 78058) and 20 mM HEPES) in a 6 well plate, and placed in the incubator (5% CO2, 37ºC) for an hour before changing to culture media without HEPES and then placed in the incubator overnight. Slices were transduced next day (DIV1) with 4mL of LNPs loaded with saRNA by directly applying onto the surface of the slice. Culture media was exchanged every 2-3 days. Z-stack images of live brain slices were acquired with an LSM 980 Airyscan 2 Confocal (Zeiss).

Statistical analysis

Mann-Whitney Ranksum tests were used to compare the area labeled between saRNA-LNPs and mRNA-LNPs (Fig. 2), and the ratio of neuron and astrocyte labeled (Fig. 3).

ACKNOWLEDGEMENTS

X. H. acknowledges funding from NIH 1RF1NS129520, 1R01NS115797, and NSF 2002971-DIOS. M.W.G. acknowledges funding from National Science Foundation TRAILBLAZER; EFMA-2421692, Boston University Kilachand Fund, and William Fairfield Warren Professorship at Boston University. W.W.W. acknowledges funding from the Boston University Kilachand Fund. D.C.S. acknowledges funding from the American Epilepsy Society Predoctoral Fellowship. J.F. acknowledges funding from NIH T32-NS136080. E.S. acknowledges funding from NIH T32-GM008764 and NIH F31 NS143166-01. J.E.M. acknowledges funding from the NSF Graduate Research Fellowship Program 2234657 and NIH T32 Translational Research in Biomaterials Training Program (T32EB006359). E. K. O. acknowledges support from pilot grant funding from the Rosamund Stone Zander and Hansjoerg Wyss Translational Neuroscience Center, Boston Children's Hospital. M. H. acknowledges funding from the Developmental Neurology Institutional Training Grant, Boston Children's Hospital, T32 NS007473. Human tissue collection was in collaboration with the Repository Core for Neurological Disorders, Boston Children's Hospital, supported IDDRC (NIH P50HD105351). This work was additionally supported by Boston University Micro and Nano Imaging Facility through NIH S10OD024993.

DATA AVAILABILITY

The data that supports the findings of this study are available upon request.

AUTHOR CONTRIBUTION

Conceptualization: WW, MWG, XH

Major data collection & analysis: JF, JEM, MH

Support for data collection and analysis: EH, SP, DS, YZ, YW, CP, LD, ESA, ZY, KL, SS, HL

Writing – Original Draft: JF, JEM, MH, JF, EKO, WW, MWG, XH

Writing – Review & Editing: All authors

Supervision: WW, MWG, XH

CONFLICT OF INTEREST

JEM, WW, and MWG hold an equity position in Keylicon Biosciences, a start-up that has licensed the modified saRNA technology from Boston University.

REFERENCES

(1) Gao, J.; Gunasekar, S.; Xia, Z. J.; Shalin, K.; Jiang, C.; Chen, H.; Lee, D.; Lee, S.; Pisal, N. D.; Luo, J. N.; et al. Gene therapy for CNS disorders: modalities, delivery and translational challenges. *Nat Rev Neurosci* **2024**, *25* (8), 553–572. DOI: 10.1038/s41583-024-00829-7 From NLM Medline.
(2) Toyoda, K.; Chu, Y.; Heistad, D. D. Gene therapy for cerebral vascular disease: update 2003. *Br J Pharmacol* **2003**, *139* (1), 1–9. DOI: 10.1038/sj.bjp.0705217 From NLM Medline.
(3) Han, X. Optogenetics in the nonhuman primate. *Prog Brain Res* **2012**, *196*, 215–233. DOI: 10.1016/B978-0-444-59426-6.00011-2.
(4) Han, X. In vivo application of optogenetics for neural circuit analysis. *ACS Chem Neurosci* **2012**, *3* (8), 577–584. DOI: 10.1021/cn300065j.
(5) Anthony, K. RNA-based therapeutics for neurological diseases. *RNA Biol* **2022**, *19* (1), 176–190. DOI: 10.1080/15476286.2021.2021650 From NLM Medline.
(6) Khare, P.; Edgecomb, S. X.; Hamadani, C. M.; Tanner, E. E. L.; D, S. M. Lipid nanoparticle-mediated drug delivery to the brain. *Advanced drug delivery reviews* **2023**, *197*, 114861. DOI: 10.1016/j.addr.2023.114861 From NLM Medline.
(7) Kariko, K.; Muramatsu, H.; Welsh, F. A.; Ludwig, J.; Kato, H.; Akira, S.; Weissman, D. Incorporation of pseudouridine into mRNA yields superior nonimmunogenic vector with increased translational capacity and biological stability. *Mol Ther* **2008**, *16* (11), 1833–1840. DOI: 10.1038/mt.2008.200 From NLM Medline.
(8) Kormann, M. S.; Hasenpusch, G.; Aneja, M. K.; Nica, G.; Flemmer, A. W.; Herber-Jonat, S.; Huppmann, M.; Mays, L. E.; Illenyi, M.; Schams, A.; et al. Expression of therapeutic proteins after delivery of chemically modified mRNA in mice. *Nat Biotechnol* **2011**, *29* (2), 154–157. DOI: 10.1038/nbt.1733 From NLM Medline.
(9) Anderson, B. R.; Muramatsu, H.; Nallagatla, S. R.; Bevilacqua, P. C.; Sansing, L. H.; Weissman, D.; Kariko, K. Incorporation of pseudouridine into mRNA enhances translation by diminishing PKR activation. *Nucleic acids research* **2010**, *38* (17), 5884–5892. DOI: 10.1093/nar/gkq347 From NLM Medline.
(10) Polack, F. P.; Thomas, S. J.; Kitchin, N.; Absalon, J.; Gurtman, A.; Lockhart, S.; Perez, J. L.; Perez Marc, G.; Moreira, E. D.; Zerbini, C.; et al. Safety and Efficacy of the BNT162b2 mRNA Covid-19 Vaccine. *N Engl J Med* **2020**, *383* (27), 2603–2615. DOI: 10.1056/NEJMoa2034577 From NLM Medline.
(11) Kariko, K.; Keller, J. M.; Harris, V. A.; Langer, D. J.; Welsh, F. A. In vivo protein expression from mRNA delivered into adult rat brain. *J Neurosci Methods* **2001**, *105* (1), 77–86. DOI: 10.1016/s0165-0270(00)00355-1 From NLM Medline.
(12) Tanaka, H.; Nakatani, T.; Furihata, T.; Tange, K.; Nakai, Y.; Yoshioka, H.; Harashima, H.; Akita, H. In Vivo Introduction of mRNA Encapsulated in Lipid Nanoparticles to Brain Neuronal Cells and Astrocytes via Intracerebroventricular Administration. *Molecular*

pharmaceutics **2018**, *15* (5), 2060–2067. DOI: 10.1021/acs.molpharmaceut.7b01084 From NLM Medline.
(13) Li, Y.; Jarvis, R.; Zhu, K.; Glass, Z.; Ogurlu, R.; Gao, P.; Li, P.; Chen, J.; Yu, Y.; Yang, Y.; et al. Protein and mRNA Delivery Enabled by Cholesteryl-Based Biodegradable Lipidoid Nanoparticles. *Angew Chem Int Ed Engl* **2020**, *59* (35), 14957–14964. DOI: 10.1002/anie.202004994 From NLM Medline.
(14) Palanki, R.; Bose, S. K.; Dave, A.; White, B. M.; Berkowitz, C.; Luks, V.; Yaqoob, F.; Han, E.; Swingle, K. L.; Menon, P.; et al. Ionizable Lipid Nanoparticles for Therapeutic Base Editing of Congenital Brain Disease. *ACS Nano* **2023**, *17* (14), 13594–13610. DOI: 10.1021/acsnano.3c02268 From NLM Medline.
(15) Xue, Y.; Wang, C.; Li, H.; Du, S.; Zhong, Y.; Zhang, Y.; Wang, S.; Guo, K.; Hou, X.; Kang, D. D.; et al. Lipid Nanoparticles Enhance mRNA Delivery to the Central Nervous System Upon Intrathecal Injection. *Adv Mater* **2025**, *37* (27), e2417097. DOI: 10.1002/adma.202417097 From NLM Medline.
(16) Kojima, R.; Bojar, D.; Rizzi, G.; Hamri, G. C.; El-Baba, M. D.; Saxena, P.; Auslander, S.; Tan, K. R.; Fussenegger, M. Designer exosomes produced by implanted cells intracerebrally deliver therapeutic cargo for Parkinson's disease treatment. *Nat Commun* **2018**, *9* (1), 1305. DOI: 10.1038/s41467-018-03733-8 From NLM Medline.
(17) Kim, M.; Oh, J.; Lee, Y.; Lee, E. H.; Ko, S. H.; Jeong, J. H.; Park, C. H.; Lee, M. Delivery of self-replicating messenger RNA into the brain for the treatment of ischemic stroke. *J Control Release* **2022**, *350*, 471–485. DOI: 10.1016/j.jconrel.2022.08.049 From NLM Medline.
(18) Minnaert, A. K.; Vanluchene, H.; Verbeke, R.; Lentacker, I.; De Smedt, S. C.; Raemdonck, K.; Sanders, N. N.; Remaut, K. Strategies for controlling the innate immune activity of conventional and self-amplifying mRNA therapeutics: Getting the message across. *Advanced drug delivery reviews* **2021**, *176*, 113900. DOI: 10.1016/j.addr.2021.113900 From NLM Medline.
(19) Kairuz, D.; Samudh, N.; Ely, A.; Arbuthnot, P.; Bloom, K. Advancing mRNA technologies for therapies and vaccines: An African context. *Front Immunol* **2022**, *13*, 1018961. DOI: 10.3389/fimmu.2022.1018961 From NLM Medline.
(20) Voigt, E. A.; Gerhardt, A.; Hanson, D.; Jennewein, M. F.; Battisti, P.; Reed, S.; Singh, J.; Mohamath, R.; Bakken, J.; Beaver, S.; et al. A self-amplifying RNA vaccine against COVID-19 with long-term room-temperature stability. *NPJ Vaccines* **2022**, *7* (1), 136. DOI: 10.1038/s41541-022-00549-y From NLM PubMed-not-MEDLINE.
(21) Beissert, T.; Perkovic, M.; Vogel, A.; Erbar, S.; Walzer, K. C.; Hempel, T.; Brill, S.; Haefner, E.; Becker, R.; Tureci, O.; et al. A Trans-amplifying RNA Vaccine Strategy for Induction of Potent Protective Immunity. *Mol Ther* **2020**, *28* (1), 119–128. DOI: 10.1016/j.ymthe.2019.09.009 From NLM Medline.
(22) Erasmus, J. H.; Archer, J.; Fuerte-Stone, J.; Khandhar, A. P.; Voigt, E.; Granger, B.; Bombardi, R. G.; Govero, J.; Tan, Q.; Durnell, L. A.; et al. Intramuscular Delivery of Replicon RNA Encoding ZIKV-117 Human Monoclonal Antibody Protects against Zika Virus Infection. *Mol Ther Methods Clin Dev* **2020**, *18*, 402–414. DOI: 10.1016/j.omtm.2020.06.011 From NLM PubMed-not-MEDLINE.

(23) Blakney, A. K.; McKay, P. F.; Christensen, D.; Yus, B. I.; Aldon, Y.; Follmann, F.; Shattock, R. J. Effects of cationic adjuvant formulation particle type, fluidity and immunomodulators on delivery and immunogenicity of saRNA. *J Control Release* **2019**, *304*, 65–74. DOI: 10.1016/j.jconrel.2019.04.043 From NLM Medline.
(24) Papukashvili, D.; Rcheulishvili, N.; Liu, C.; Ji, Y.; He, Y.; Wang, P. G. Self-Amplifying RNA Approach for Protein Replacement Therapy. *International journal of molecular sciences* **2022**, *23* (21). DOI: 10.3390/ijms232112884 From NLM Medline.
(25) Kairuz, D.; Samudh, N.; Ely, A.; Arbuthnot, P.; Bloom, K. Production, Characterization, and Assessment of Permanently Cationic and Ionizable Lipid Nanoparticles for Use in the Delivery of Self-Amplifying RNA Vaccines. *Pharmaceutics* **2023**, *15* (4). DOI: 10.3390/pharmaceutics15041173 From NLM PubMed-not-MEDLINE.
(26) Deering, R. P.; Kommareddy, S.; Ulmer, J. B.; Brito, L. A.; Geall, A. J. Nucleic acid vaccines: prospects for non-viral delivery of mRNA vaccines. *Expert Opin Drug Deliv* **2014**, *11* (6), 885–899. DOI: 10.1517/17425247.2014.901308 From NLM Medline.
(27) Pollock, K. M.; Cheeseman, H. M.; Szubert, A. J.; Libri, V.; Boffito, M.; Owen, D.; Bern, H.; O'Hara, J.; McFarlane, L. R.; Lemm, N. M.; et al. Safety and immunogenicity of a self-amplifying RNA vaccine against COVID-19: COVAC1, a phase I, dose-ranging trial. *EClinicalMedicine* **2022**, *44*, 101262. DOI: 10.1016/j.eclinm.2021.101262 From NLM PubMed-not-MEDLINE.
(28) McGee, J. E.; Kirsch, J. R.; Kenney, D.; Cerbo, F.; Chavez, E. C.; Shih, T. Y.; Douam, F.; Wong, W. W.; Grinstaff, M. W. Complete substitution with modified nucleotides in self-amplifying RNA suppresses the interferon response and increases potency. *Nat Biotechnol* **2024**. DOI: 10.1038/s41587-024-02306-z From NLM Publisher.
(29) Han, X.; Zhang, H.; Butowska, K.; Swingle, K. L.; Alameh, M. G.; Weissman, D.; Mitchell, M. J. An ionizable lipid toolbox for RNA delivery. *Nat Commun* **2021**, *12* (1), 7233. DOI: 10.1038/s41467-021-27493-0 From NLM Medline.
(30) Hou, X.; Zaks, T.; Langer, R.; Dong, Y. Lipid nanoparticles for mRNA delivery. *Nat Rev Mater* **2021**, *6* (12), 1078–1094. DOI: 10.1038/s41578-021-00358-0 From NLM PubMed-not-MEDLINE.
(31) Luo, D.; Saltzman, W. M. Synthetic DNA delivery systems. *Nat Biotechnol* **2000**, *18* (1), 33–37, Research Support, U.S. Gov't, P.H.S.

Review. DOI: 10.1038/71889.
(32) Tuma, J.; Chen, Y. J.; Collins, M. G.; Paul, A.; Li, J.; Han, H.; Sharma, R.; Murthy, N.; Lee, H. Y. Lipid Nanoparticles Deliver mRNA to the Brain after an Intracerebral Injection. *Biochemistry* **2023**, *62* (24), 3533–3547. DOI: 10.1021/acs.biochem.3c00371 From NLM Medline.
(33) Raguram, A.; Banskota, S.; Liu, D. R. Therapeutic in vivo delivery of gene editing agents. *Cell* **2022**, *185* (15), 2806–2827. DOI: 10.1016/j.cell.2022.03.045 From NLM Medline.
(34) Han, E. L.; Padilla, M. S.; Palanki, R.; Kim, D.; Mrksich, K.; Li, J. J.; Tang, S.; Yoon, I. C.; Mitchell, M. J. Predictive High-Throughput Platform for Dual Screening of mRNA Lipid Nanoparticle Blood-Brain Barrier Transfection and Crossing. *Nano Lett* **2024**, *24* (5), 1477–1486. DOI: 10.1021/acs.nanolett.3c03509 From NLM Medline.

(35) Kim, J.; Eygeris, Y.; Ryals, R. C.; Jozic, A.; Sahay, G. Strategies for non-viral vectors targeting organs beyond the liver. *Nat Nanotechnol* **2024**, *19* (4), 428–447. DOI: 10.1038/s41565-023-01563-4 From NLM Medline.
(36) Li, H.; Cao, Y.; Ye, J.; Yang, Z.; Chen, Q.; Liu, X.; Zhang, B.; Qiao, J.; Tang, Q.; Yang, H.; et al. Engineering brain-derived neurotrophic factor mRNA delivery for the treatment of Alzheimer's disease. *Chemical Engineering Journal* **2023**, *466*, 143152. DOI: https://doi.org/10.1016/j.cej.2023.143152.
(37) Sela, M.; Chen, G.; Kadosh, H.; Kagan, T.; Nicola, R.; Turutov, S.; Richtman, Y.; Zhige, L.; Albalak Menasherov, M. R.; Kagan, S.; et al. AI-Validated Brain Targeted mRNA Lipid Nanoparticles with Neuronal Tropism. *ACS Nano* **2025**, *19* (41), 36106–36128. DOI: 10.1021/acsnano.4c15013 From NLM Medline.
(38) Bleier, B. S.; Kohman, R. E.; Guerra, K.; Nocera, A. L.; Ramanlal, S.; Kocharyan, A. H.; Curry, W. T.; Han, X. Heterotopic Mucosal Grafting Enables the Delivery of Therapeutic Neuropeptides Across the Blood Brain Barrier. *Neurosurgery* **2016**, *78* (3), 448–457; discussion 457. DOI: 10.1227/NEU.0000000000001016.
(39) Lawrence, M. S.; McLaughlin, J. R.; Sun, G. H.; Ho, D. Y.; McIntosh, L.; Kunis, D. M.; Sapolsky, R. M.; Steinberg, G. K. Herpes simplex viral vectors expressing Bcl-2 are neuroprotective when delivered after a stroke. *J Cereb Blood Flow Metab* **1997**, *17* (7), 740–744. DOI: 10.1097/00004647-199707000-00003 From NLM Medline.
(40) Peng, H.; Guo, X.; He, J.; Duan, C.; Yang, M.; Zhang, X.; Zhang, L.; Fu, R.; Wang, B.; Wang, D.; et al. Intracranial delivery of synthetic mRNA to suppress glioblastoma. *Mol Ther Oncolytics* **2022**, *24*, 160–170. DOI: 10.1016/j.omto.2021.12.010 From NLM PubMed-not-MEDLINE.
(41) Marcos-Contreras, O. A.; Greineder, C. F.; Kiseleva, R. Y.; Parhiz, H.; Walsh, L. R.; Zuluaga-Ramirez, V.; Myerson, J. W.; Hood, E. D.; Villa, C. H.; Tombacz, I.; et al. Selective targeting of nanomedicine to inflamed cerebral vasculature to enhance the blood-brain barrier. *Proc Natl Acad Sci U S A* **2020**, *117* (7), 3405–3414. DOI: 10.1073/pnas.1912012117 From NLM Medline.
(42) Shyam, R.; Ren, Y.; Lee, J.; Braunstein, K. E.; Mao, H. Q.; Wong, P. C. Intraventricular Delivery of siRNA Nanoparticles to the Central Nervous System. *Mol Ther Nucleic Acids* **2015**, *4*, e242. DOI: 10.1038/mtna.2015.15 From NLM PubMed-not-MEDLINE.
(43) Yang, X.; Yang, W.; Xia, X.; Lei, T.; Yang, Z.; Jia, W.; Zhou, Y.; Cheng, G.; Gao, H. Intranasal Delivery of BACE1 siRNA and Rapamycin by Dual Targets Modified Nanoparticles for Alzheimer's Disease Therapy. *Small* **2022**, *18* (30), e2203182. DOI: 10.1002/smll.202203182 From NLM Medline.
(44) Wang, P.; Zheng, X.; Guo, Q.; Yang, P.; Pang, X.; Qian, K.; Lu, W.; Zhang, Q.; Jiang, X. Systemic delivery of BACE1 siRNA through neuron-targeted nanocomplexes for treatment of Alzheimer's disease. *J Control Release* **2018**, *279*, 220–233. DOI: 10.1016/j.jconrel.2018.04.034 From NLM Medline.
(45) Zhou, Y.; Zhu, F.; Liu, Y.; Zheng, M.; Wang, Y.; Zhang, D.; Anraku, Y.; Zou, Y.; Li, J.; Wu, H.; et al. Blood-brain barrier-penetrating siRNA nanomedicine for Alzheimer's disease therapy. *Sci Adv* **2020**, *6* (41). DOI: 10.1126/sciadv.abc7031 From NLM Medline.
(46) Helmschrodt, C.; Hobel, S.; Schoniger, S.; Bauer, A.; Bonicelli, J.; Gringmuth, M.; Fietz, S. A.; Aigner, A.; Richter, A.; Richter, F. Polyethylenimine Nanoparticle-Mediated siRNA

Delivery to Reduce alpha-Synuclein Expression in a Model of Parkinson's Disease. *Mol Ther Nucleic Acids* **2017**, *9*, 57–68. DOI: 10.1016/j.omtn.2017.08.013 From NLM PubMed-not-MEDLINE.
(47) Schlich, M.; Longhena, F.; Faustini, G.; O'Driscoll, C. M.; Sinico, C.; Fadda, A. M.; Bellucci, A.; Lai, F. Anionic liposomes for small interfering ribonucleic acid (siRNA) delivery to primary neuronal cells: Evaluation of alpha-synuclein knockdown efficacy. *Nano Research* **2017**, *10* (10), 3496–3508. DOI: 10.1007/s12274-017-1561-z.
(48) Xie, Q.; Li, K.; Chen, Y.; Li, Y.; Jiang, W.; Cao, W.; Yu, H.; Fan, D.; Deng, B. Gene therapy breakthroughs in ALS: a beacon of hope for 20% of ALS patients. *Transl Neurodegener* **2025**, *14* (1), 19. DOI: 10.1186/s40035-025-00477-6 From NLM Medline.
(49) Liu, S.; Liu, J.; Li, H.; Mao, K.; Wang, H.; Meng, X.; Wang, J.; Wu, C.; Chen, H.; Wang, X.; et al. An optimized ionizable cationic lipid for brain tumor-targeted siRNA delivery and glioblastoma immunotherapy. *Biomaterials* **2022**, *287*, 121645. DOI: 10.1016/j.biomaterials.2022.121645 From NLM Publisher.
(50) Rosenblum, D.; Gutkin, A.; Kedmi, R.; Ramishetti, S.; Veiga, N.; Jacobi, A. M.; Schubert, M. S.; Friedmann-Morvinski, D.; Cohen, Z. R.; Behlke, M. A.; et al. CRISPR-Cas9 genome editing using targeted lipid nanoparticles for cancer therapy. *Sci Adv* **2020**, *6* (47). DOI: 10.1126/sciadv.abc9450 From NLM Medline.
(51) Baiersdorfer, M.; Boros, G.; Muramatsu, H.; Mahiny, A.; Vlatkovic, I.; Sahin, U.; Kariko, K. A Facile Method for the Removal of dsRNA Contaminant from In Vitro-Transcribed mRNA. *Mol Ther Nucleic Acids* **2019**, *15*, 26–35. DOI: 10.1016/j.omtn.2019.02.018 From NLM PubMed-not-MEDLINE.

SUPPLEMENTAL FIGURES

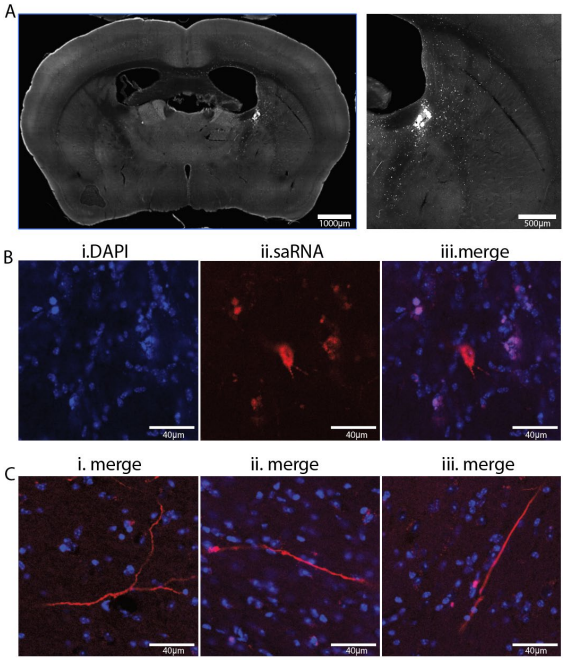

Supplemental Figure 1. saRNA-LNP demonstrates robust mCherry expression in some neurons at 3 months post injection. (A) Left; An example brain slice showing saRNA-LNP mediated mCherry expression at 3 months post-injection. Right; A zoom-in view around the injection site. **(B)** saRNA-LNP labeled cell bodies. (i) DAPI fluorescence (blue) indicating cell nuclei; (ii) saRNA-LNP mediated mCherry fluorescence; (iii) merge. (**C**) saRNA-LNP labeled neuronal processes. Shown are three example neurites (red, mCherry fluorescence), co-stained with DAPI fluorescence (blue).

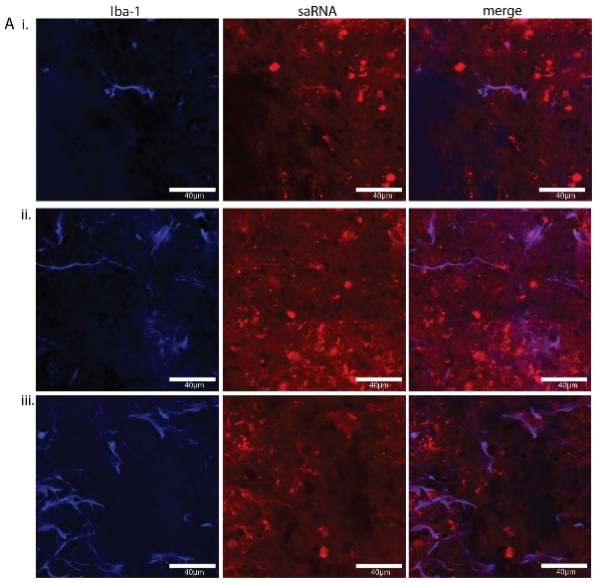

Supplemental Figure 2. saRNA-LNP mediated mCherry expression in microglia. (Ai-iii) 3 example fields of view at 1-week post injection. Left, Iba-1 immunofluorescence (blue); middle, saRNA mediated mCherry expression (red), right, merge.